

# Action at a Distance: Amino Acid Substitutions That Affect Binding of the Phosphorylated CheY Response Regulator and Catalysis of Dephosphorylation Can Be Far from the CheZ Phosphatase Active Site<sup>∇</sup>

Ashalla M. Freeman,<sup>†</sup> Beth M. Mole,<sup>‡</sup> Ruth E. Silversmith, and Robert B. Bourret\*

Department of Microbiology and Immunology, University of North Carolina, Chapel Hill, North Carolina 27599-7290

Received 14 January 2011/Accepted 1 July 2011

**Two-component regulatory systems, in which phosphorylation controls the activity of a response regulator protein, provide signal transduction in bacteria. For example, the phosphorylated CheY response regulator (CheYp) controls swimming behavior. In *Escherichia coli*, the chemotaxis phosphatase CheZ stimulates the dephosphorylation of CheYp. CheYp apparently binds first to the C terminus of CheZ and then binds to the active site where dephosphorylation occurs. The phosphatase activity of the CheZ<sub>2</sub> dimer exhibits a positively cooperative dependence on CheYp concentration, apparently because the binding of the first CheYp to CheZ<sub>2</sub> is inhibited compared to the binding of the second CheYp. Thus, CheZ phosphatase activity is reduced at low CheYp concentrations. The CheZ21IT gain-of-function substitution, located far from either the CheZ active site or C-terminal CheY binding site, enhances CheYp binding and abolishes cooperativity. To further explore mechanisms regulating CheZ activity, we isolated 10 intragenic suppressor mutations of *cheZ21IT* that restored chemotaxis. The suppressor substitutions were located along the central portion of CheZ and were not allele specific. Five suppressor mutants tested biochemically diminished the binding of CheYp and/or the catalysis of dephosphorylation, even when the suppressor substitutions were distant from the active site. One suppressor mutant also restored cooperativity to CheZ21IT. Consideration of results from this and previous studies suggests that the binding of CheYp to the CheZ active site (not to the C terminus) is rate limiting and leads to cooperative phosphatase activity. Furthermore, amino acid substitutions distant from the active site can affect CheZ catalytic activity and CheYp binding, perhaps via the propagation of structural or dynamic perturbations through a helical bundle.**

Transient protein phosphorylation is a common means to accomplish signal transduction. Phosphorylation-mediated signaling in microorganisms often involves the detection of a stimulus by a sensor kinase, followed by the transfer of a phosphoryl group to a response regulator protein. In bacterial chemotaxis, one of the best-studied examples of such a two-component regulatory system (36, 37), extracellular stimuli control the autophosphorylation of the CheA sensor kinase with subsequent phosphotransfer to the cytoplasmic response regulator CheY. The phosphorylation state of CheY then dictates the direction or duration of flagellar rotation and thus swimming behavior.

The concentration of phosphorylated CheY (CheYp) at any given time is a function of the rates of both phosphorylation and dephosphorylation. The kinetics of phosphoryl group addition and removal set an upper bound on how quickly a cell can respond to a stimulus. During chemotaxis, bacteria integrate information about their chemical environment and make

split-second responses that determine whether to continue on their current course or change direction (29). Accordingly, CheY proteins from various species have among the fastest known rates of self-catalyzed dephosphorylation for response regulators (39). Nevertheless, in many bacteria CheY auto-dephosphorylation is too slow to support chemotaxis, so phosphatases of the CheZ or CheC/CheX/FliY families further stimulate the rate of removal of the phosphoryl group from CheYp. CheZ and CheX exhibit little similarity in structure or amino acid sequence but use the same mechanism to accelerate CheYp dephosphorylation (22, 24, 30, 41). The present study explores amino acid substitutions that perturb CheZ activity and potentially provide insight into phosphatase regulation.

The structure of *Escherichia coli* CheZ cocrystallized with CheY and the stable phosphoryl group analog BeF<sub>3</sub><sup>-</sup> (41) revealed basic features of CheZ architecture and the mechanism of CheZ-mediated CheYp dephosphorylation. CheZ is a highly helical, homodimeric protein that binds two CheYp molecules. The CheZ dimer forms a long (>100-Å) four-helix bundle consisting of amphipathic helices that fold into a hairpin structure (Fig. 1). Two additional alpha helices are present in each CheZ monomer. One helix at the N terminus of CheZ (N helix; residues 1 to 34) connects directly to the four-helix bundle, whereas the other helix, located at the C terminus of CheZ (C helix; residues 199 to 214), is tethered to the bundle by a 32-residue highly flexible linker (31, 41).

\* Corresponding author. Mailing address: Department of Microbiology and Immunology, University of North Carolina, Chapel Hill, NC 27599-7290. Phone: (919) 966-2679. Fax: (919) 962-8103. E-mail: bourret@med.unc.edu.

<sup>†</sup> Present address: Biological and Biomedical Sciences Program, University of North Carolina, Chapel Hill, NC 27599-7108.

<sup>‡</sup> Present address: Division of Medicinal Chemistry and Natural Products, University of North Carolina, Chapel Hill, NC 27599-7568.

<sup>∇</sup> Published ahead of print on 15 July 2011.

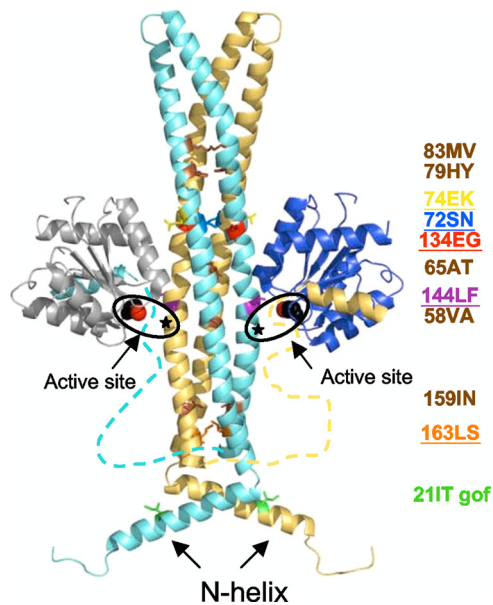


FIG. 1. Ribbon diagram of the CheY · CheZ cocystal structure (Protein Data Bank accession number 1KMI). The two chains composing the CheZ dimer are in cyan and gold, and the two CheY molecules are in blue and gray. The locations of the CheZ21IT GOF substitution as well as suppressor substitutions are drawn as sticks on the ribbon diagram and listed in matching colors. Suppressor substitutions chosen for biochemical analysis are underlined.  $\text{BeF}_3^-$  (non-hydrolyzable phosphoryl group analog) and  $\text{Mg}^{2+}$  are indicated as black and red spheres, respectively, and the locations of the CheZ catalytic Gln147 residues are indicated as black stars. The N helix and active sites of both CheZ chains also are indicated. The flexible linkers, which were disordered in the cocystal structure (41), are sketched as dotted lines.

Each CheYp interacts with CheZ at two distinct sites: the C helix (2, 11, 12, 20, 41) and the CheZ active-site region near the center of the four-helix bundle (41). In the latter interaction, the essential catalytic residue Gln147 inserts into the CheYp active site (Fig. 1). In a current model of the CheZ-mediated dephosphorylation of CheYp, CheYp is believed to initially bind to the C helix of CheZ (31, 32). Following this initial interaction, CheYp is tethered to the four-helix bundle via the flexible linker, which brings the CheYp active site in closer proximity to the CheZ catalytic residue Gln147 and thus leads to CheYp dephosphorylation (31). The rate of the CheZ-mediated dephosphorylation of CheYp exhibits positive cooperativity (sigmoidal curve) with respect to CheYp concentration (3, 32). The positive cooperativity is consistent with a model whereby there is a slower association of CheYp with uncomplexed CheZ<sub>2</sub> relative to the rate of association of CheYp with CheZ<sub>2</sub> · CheYp. Positive cooperativity could serve as a mechanism to limit CheZ activity when the CheYp concentration is low (32).

CheZ residues outside the active site and sites of CheYp interaction also impact phosphatase activity. In particular, amino acid substitutions that increase phosphatase activity (15, 25, 26, 35) cluster along the N helix and the nearby region of the four-helix bundle (Fig. 1) (41). One such gain-of-function (GOF) mutation, *cheZ21IT*, has been the subject of significant study. Although CheZ21IT exhibits a  $k_{\text{cat}}$  similar to that of

wild-type CheZ (32), CheZ21IT does not support chemotaxis (26). A loss of the positive cooperativity observed for wild-type CheZ means that CheZ21IT has increased phosphatase activity at low CheYp concentrations and reaches half-maximal activity at a 4-fold lower CheYp concentration than wild-type CheZ (32). Moreover, CheZ21IT has a rate constant of association with CheYp that is 6-fold faster than that for wild-type CheZ and a rate constant of dissociation from CheYp that is 1.7-fold slower than that for wild-type CheZ, and hence it binds CheYp with 10-fold greater affinity ( $K_d$  of 0.68 nM) than wild-type CheZ ( $K_d$  of 7.1 nM) (32).

The observation that the CheZ21IT substitution located on the N helix more than 40 Å from the active site does not support chemotaxis and abolishes the positive cooperativity of phosphatase activity without affecting  $k_{\text{cat}}$  (32) is consistent with the possibility that there are as-yet unidentified interactions within CheZ that influence the dephosphorylation of CheYp. The means by which residues so distant from the CheZ active site and sites of CheYp interaction affect phosphatase activity might involve structural changes that propagate along the four-helix bundle to alter the properties of the active-site region. Alternatively, perturbed packing interactions between the N helix, four-helix bundle, flexible linker, and/or C helix of CheZ could influence CheYp binding to the C helix. Here, we identified and characterized intragenic suppressors of *cheZ21IT* to investigate the mechanism by which distant residues alter phosphatase activity and disrupt positive cooperativity. Taken together, the results of this and other studies suggest that the binding of CheYp to the CheZ active site is the rate-limiting step in association with CheYp and the source of CheZ cooperativity.

## MATERIALS AND METHODS

**Site-directed mutagenesis.** Site-specific mutations were generated using the QuikChange site-directed mutagenesis kit (Stratagene) according to the manufacturer's instructions. The GOF mutation *cheZ21IT* was generated in plasmid pRS3 (31). Like its predecessor, the ampicillin-resistant pBR322 derivative pRBB40 (5), pRS3 contains a 2.6-kb BamHI-HindIII fragment encoding '*cheBYZ, flhB*'; however, the *cheZ134EK* mutation present in pRBB40 (4) has been corrected in pRS3. The mutagenic primer used to generate *cheZ21IT* contained changes at two of the nucleotides encoding residue 21 to eliminate the possibility that the reversion of the GOF mutation could occur after a single base change, thus favoring the isolation of second-site suppressors rather than revertants in the screen for the restoration of chemotaxis. Plasmids carrying only the suppressor mutation were constructed by correcting the *cheZ21IT* mutation back to the wild type in plasmids containing both *cheZ21IT* and a suppressor mutation (described below). To assess the allele specificity of suppression, the gain-of-function mutation *cheZ24LP* subsequently was introduced into pRS3 and plasmids containing only a suppressor mutation. Plasmids potentially carrying *cheZ21IT*, *cheZ24LP*, and/or *cheZ* suppressor mutations from the constructions described above were isolated from ampicillin-resistant transformants, and the *cheYZ* genes were sequenced. Plasmids containing wild-type *cheY* and the desired *cheZ* mutations were transformed into the  $\Delta$ *cheYZ* strain RP5231, and the resultant strains were characterized with a motility plate assay (described below). RP5231, derived from the wild-type chemotaxis strain RP437 (23), carries  $\Delta$ *cheYZ4313* (18) and was a gift from J. S. Parkinson.

**Suppressor generation and isolation.** To generate suppressor mutations of *cheZ21IT*, pRS3 containing *cheZ21IT* was transformed into NR9458 (27) cells rendered chemically competent following growth in minimal media as described previously (4). NR9458 carries the *mutD5* allele and exhibits increased mutation frequencies (50 to 100 times higher than that of the wild type) when grown in minimal medium (9). Transformation cultures of the mutagenic NR9458 strain were grown overnight, and the resulting library of plasmids was isolated and subsequently transformed into the motility assay strain RP5231. A 100- $\mu$ l sample of the RP5231 transformation mix was diluted into 5 ml of LB broth with

ampicillin and again grown overnight. To screen for suppressors, 20  $\mu$ l of the overnight culture of RP5231 carrying mutagenized pRS3.cheZ21IT was streaked across the center of motility agar (1% [wt/vol] tryptone, 0.5% [wt/vol] NaCl, 0.3% [wt/vol] BactoAgar) plates and incubated overnight at 30°C. Transformants were screened for the normal chemotactic behavior of radial growth pattern from the inoculation site accompanied by swarm ring formation, in contrast to the CheZ GOF mutant nonchemotactic phenotype. Potential suppressor mutants were picked from the swarm rings, single-colony purified, and assayed in a motility plate assay (described below) to confirm swarm phenotypes. Plasmid DNA from candidate suppressor mutants was isolated, and the *cheYZ* genes were sequenced. Plasmids containing only *cheZ* point mutations in addition to *cheZ21IT* were retransformed into RP5231 to confirm that the swarm phenotypes were linked to the plasmid and not the result of spontaneous chromosomal mutations. To confirm that the swarm phenotypes were due to mutations in *cheZ*, the *cheZ* gene from plasmids containing *cheZ* double (*cheZ21IT* and suppressor) mutations was subcloned into nonmutagenized pRS3. Plasmids were double digested with PvuII and Bsu36I, which both cleave within *cheZ*, and the fragments were separated by agarose gel electrophoresis. Because PvuII cleaves at ~40 bp and Bsu36I cleaves at ~80 bp from the 5' and 3' ends of *cheZ*, respectively, the 0.5-kb DNA fragment generated following double digestion includes the codon for position 21 and all of the suppressor mutations. This 0.5-kb fragment was gel purified and ligated into the PvuII/Bsu36I sites of pRS3 that had been treated with calf intestinal alkaline phosphatase (Promega) using the rapid DNA ligation kit (Roche) according to the manufacturer's instructions. Ten- $\mu$ l samples of the ligation reactions were transformed into Max Efficiency DH5 $\alpha$ -competent cells (Invitrogen). Plasmids were isolated from ampicillin-resistant transformants, the *cheYZ* genes were sequenced from plasmids of the correct size (~4.8 kb), and those containing *cheZ* double mutations and wild-type *cheY* were transformed into RP5231. The resulting strains were subjected to a motility plate assay (described below).

**Chemotaxis assay.** The standard motility plate assay was performed as described previously (1). Briefly, single bacterial colonies were stabbed into motility agar plates and incubated at 30°C for approximately 8 h. Swarm diameters were measured throughout the growth period, and growth rates (in mm/h) after the lag phase were determined and compared to those of swarms generated by chemotactic (RP5231/pRS3) and nonchemotactic (RP5231) control strains on the same plate.

**Protein purification.** Wild-type and mutant CheZ proteins and CheY113AP were overexpressed and purified according to previously published procedures (14, 32, 33). Briefly, following the overexpression of CheY and CheZ proteins encoded on plasmids in KO642*recA* ( $\Delta$ *cheZ6725*) (6), RP5231 ( $\Delta$ *cheYZ4313*), or KO641*recA* ( $\Delta$ *cheY6021*) (5), crude lysates were applied to an Affi-Gel blue gel (Bio-Rad) column matrix, which binds CheY. CheZ does not bind Affi-Gel blue gel and was collected in the flowthrough, precipitated with (NH<sub>4</sub>)<sub>2</sub>SO<sub>4</sub>, resuspended in 50 mM Tris, pH 7.5, 0.5 mM EDTA, 10% (vol/vol) glycerol, and chromatographed on a 5 ml Hi-Trap Q Sepharose FF column (GE Healthcare). CheZ-containing fractions were pooled and concentrated to  $\leq$ 5 ml, chromatographed on a Superose-12 (GE Healthcare) fast-protein liquid chromatography (FPLC) gel filtration column, and finally concentrated and stored at -70°C. Each purified CheZ protein yielded a gel filtration peak corresponding to a dimer; no CheZ monomers were observed. For CheY113AP purification, CheY was eluted from the Affi-Gel column using a high-salt buffer, dialyzed, applied to a DEAE cellulose (DE52; Whatman) anion exchange column, and again eluted with a high-salt buffer. CheY-containing fractions were pooled and concentrated to  $\approx$ 5 ml, chromatographed on a Superose-12 (GE Healthcare) FPLC gel filtration column, and finally concentrated and stored at -20°C. Prior to storage, the concentrations of CheY and CheZ were determined by measuring the absorbance at 280 nm and using empirically determined extinction coefficients of 0.73 (mg/ml)<sup>-1</sup> cm<sup>-1</sup> and 0.70 (mg/ml)<sup>-1</sup> cm<sup>-1</sup> (33), respectively.

**Western blot analysis.** Strains were grown to exponential phase (optical density at 600 nm of ~0.6 to 0.7) in LB, and 1-ml samples were harvested by centrifugation. Pellets were resuspended in 1 ml of wash buffer (50 mM Tris-HCl, 0.5 mM EDTA, 2 mM dithiothreitol, 10% [vol/vol] glycerol, pH 7.5) and centrifuged again. The supernatant was removed and pellets were stored at -20°C for later use. To prepare crude lysates for SDS-PAGE analysis, pellets were thawed, resuspended in 100 to 150  $\mu$ l of 1% (wt/vol) SDS, and boiled for 6 min. The total protein concentration was measured using the Micro-bicinchoninic acid (BCA) protein assay kit (Pierce) according to the manufacturer's microplate procedure with the following changes: 5 to 15  $\mu$ l of crude lysate was diluted to a final volume of 150  $\mu$ l in sterile deionized H<sub>2</sub>O in microcentrifuge tubes; following the addition of the BCA kit reagent, reaction mixtures were incubated for 1 h at 60°C and then transferred to a 96-well microtiter plate for the measure-

ment of the absorbance at 562 nm. Total protein concentrations of the crude lysates ranged from ~1 to 1.5 mg/ml.

For the SDS-PAGE analysis of the crude lysates, 2 $\times$  sample buffer (125 mM Tris, pH 6.8, 4% [vol/vol] SDS, 20% [vol/vol] glycerol, 10% [vol/vol] 2-mercaptoethanol, 0.02% [wt/vol] bromophenol blue) was added to 15  $\mu$ g of total protein to a final volume of  $\leq$ 25  $\mu$ l, mixed, boiled for 6 min, and loaded immediately onto a 4 to 20% (Tris-HEPES-SDS) Precise protein gel (Pierce). Gels were electrophoresed and transferred onto nitrocellulose membranes according to the gel manufacturer's instructions using the wet blotting protocol.

Membranes were blocked, washed, probed, and developed according to standard Western blotting protocols (38). Antibodies were diluted in phosphate-buffered saline containing 0.1% (vol/vol) Tween 20 at the following concentrations: anti-CheZ polyclonal rabbit antisera (kind gift of Philip Matsumura) diluted 1/1,000 and goat-anti-rabbit IgG (whole molecule)-peroxidase antibody (Sigma) diluted 1/15,000. Detection was achieved using the ECL Western blotting substrate (Pierce) according to the manufacturer's instructions. The intensities of detected bands were compared visually.

**Phosphatase activity measurements.** Purified wild-type and mutant CheZ proteins were assessed for the ability to dephosphorylate CheY113AP using the EnzChek phosphate assay kit (Molecular Probes) adapted to a 96-well plate format according to previously published procedures (32, 33). CheY113AP was used as the substrate because it has an enhanced autophosphorylation rate (34), resulting in increased rates of P<sub>i</sub> release in the presence of excess CheZ, which augments the range of dephosphorylation rates that can be measured at low CheY concentrations (32). Briefly, in a 96-well flat-bottomed polystyrene microtiter plate (Greiner Bio-One), various amounts of CheY113AP were mixed with 50 to 52.5 nM CheZ in buffer containing 50 mM HEPES, pH 7.0, 10 mM MgCl<sub>2</sub>, and 1 mg/ml bovine serum albumin. Reactions were started by the addition of the phosphodonor monophosphoimidazole (MPI) to a final concentration of 4 mM. The autophosphorylation of CheY113AP with MPI generates the CheY113APP substrate for the CheZ-mediated dephosphorylation reaction. Immediately following the addition of MPI, reaction solutions were mixed by repetitive pipetting and covered to prevent sample loss during the 44-min incubation at room temperature. Reactions were quenched by the addition of 250 mM Tris-HCl, pH 7.5, 25 mM EDTA, 310  $\mu$ M 2-amino-6-mercapto-7-methylpurine riboside, and 1.4 U/ml purine nucleoside phosphorylase. After an incubation of at least 15 min, P<sub>i</sub> was detected by measuring the absorbance at 360 nm in a SpectraMax M2<sup>e</sup> microplate reader (Molecular Devices). Absorbances were converted to P<sub>i</sub> release rates ( $\mu$ M P<sub>i</sub>/s) using an extinction coefficient derived from a P<sub>i</sub> standard curve included on each plate. The data were processed as described previously (32). (i) P<sub>i</sub> release rates were corrected for contaminating P<sub>i</sub> in the MPI using experimental controls lacking CheY113AP. (ii) The rate constant for phosphorylation was determined using experimental controls in the presence of CheY113AP and excess CheZ. (iii) The concentration of nonphosphorylated CheY113AP was calculated using the rate constant for phosphorylation and the observed rate of P<sub>i</sub> release. (iv) The concentration of CheY113APP was calculated by the subtraction of nonphosphorylated CheY113AP from total CheY113AP. (v) P<sub>i</sub> release due to CheZ was determined by subtracting the amount of P<sub>i</sub> released in the absence of CheZ from the observed rate. (vi) At low concentrations of CheY113APP, CheZ-mediated P<sub>i</sub> release is small compared to background P<sub>i</sub> from the phosphodonor (step i) or CheY autodephosphorylation (step v). The error inherent in the small difference between two large numbers occasionally resulted in a negative value for the calculated CheZ-mediated P<sub>i</sub> release. In such circumstances, a fixed correction sufficient to bring the rate of the lowest point up to zero was added to each data point in the set. The largest correction applied to any set was 0.0085  $\mu$ M/s, which corresponds to 0.17 s<sup>-1</sup> in *k*<sub>cat</sub> values. Each reaction condition was assayed in duplicate wells, and duplicate data from independent experiments were averaged to obtain the kinetic values.

The calculated CheZ-stimulated P<sub>i</sub> release rate was plotted as a function of calculated CheY113APP concentration, and the data were fit by nonlinear regression to the Hill equation (32) using Prism (GraphPad Software):  $v = (V_{\max} [\text{CheYp}]^n) / (K_{1/2n} + [\text{CheYp}]^n)$ , where  $V_{\max}$  [CheYp] (the maximum velocity of P<sub>i</sub> release stimulated by CheZ),  $K_{1/2}$  (the concentration of CheYp necessary for half-maximal velocity), and  $n$  (the Hill coefficient) are floating variables.  $k_{\text{cat}}$  (the catalytic rate constant) was determined using the following equation:  $k_{\text{cat}} = V_{\max} / [\text{CheZ}]$ .

Some proteins exhibited apparent Hill coefficients above the usual maximum value of 2 for a dimeric enzyme. The phenomenon of zero-order ultrasensitivity (10), which can lead to aberrantly high Hill coefficients, does not apply to our measurements of CheZ activity. Our mathematical modeling (not shown) similarly indicates that the nonequilibrium aspect of CheZ function, in which the dissociation of CheYp from CheZ is 1,000 times slower than the catalysis of dephosphorylation (32), does not result in unusual Hill coefficients. Instead, it

TABLE 1. Chemotactic swarm rates<sup>a</sup> of CheZ mutants containing substitutions that suppress *cheZ21IT*

Suppressor substitution <sup>b</sup>	Single mutant		Double mutant with 21IT		Double mutant with 24LP	
	Swarm rate (%)	Ring formation	Swarm rate (%)	Ring formation	Swarm rate (%)	Ring formation
83MV	82 ± 6	Che <sup>+</sup>	78 ± 0	Che <sup>+</sup>	80 ± 7	Che <sup>+</sup>
79HY	87 ± 1	Che <sup>+</sup>	77 ± 2	Che <sup>+</sup>	100 ± 2	Che <sup>+</sup>
74EK <sup>c</sup>	5.1 ± 3	Che <sup>-</sup>	96 ± 4	Che <sup>+</sup>	82 ± 2	Che <sup>+</sup>
72SN <sup>c</sup>	41 ± 1	Che <sup>-</sup>	110 ± 3	Che <sup>+</sup>	47 ± 5	Che <sup>-</sup>
134EG <sup>c</sup>	79 ± 4	Che <sup>+</sup>	97 ± 3	Che <sup>+</sup>	93 ± 10	Che <sup>+</sup>
65AT	8.1 ± 0.9	Che <sup>-</sup>	100 ± 7	Che <sup>+</sup>	80 ± 7	Che <sup>+</sup>
144LF <sup>c</sup>	16 ± 1	Che <sup>-</sup>	95 ± 10	Che <sup>+</sup>	96 ± 8	Che <sup>+</sup>
58VA	75 ± 1	Che <sup>+</sup>	87 ± 0	Che <sup>+</sup>	75 ± 6	Che <sup>+</sup>
159IN	98 ± 1	Che <sup>+</sup>	94 ± 1	Che <sup>+</sup>	94 ± 8	Che <sup>+</sup>
163LS <sup>c</sup>	84 ± 8	Che <sup>+</sup>	83 ± 2	Che <sup>+</sup>	100 ± 5	Che <sup>+</sup>
None	100	Che <sup>+</sup>	17 ± 4	Che <sup>-</sup>	25 ± 1	Che <sup>-</sup>

<sup>a</sup> The rate (mm/h) at which bacteria migrated through the agar was measured and is expressed as the percentage of the positive control strain ± standard deviations. Swarm rates for the positive (RP5231/pRS3) and negative (RP5231) control strains were 100% and 4.9% ± 3%, respectively. The average swarm rate measured for the positive control was 3.8 ± 0.7 mm/h. The formation of swarm rings indicates chemotaxis (Che<sup>+</sup>, chemotactic; Che<sup>-</sup>, nonchemotactic).

<sup>b</sup> Substitutions are listed based on their location on the four-helix bundle of CheZ (Fig. 1).

<sup>c</sup> Mutants chosen for biochemical analysis.

appears that uncertainties arising from the extensive processing of P<sub>i</sub> release assay data could be responsible for errors in the determination of Hill coefficients. The apparent Hill coefficient is particularly sensitive to variation in the ~10 points that comprise the data set for each CheZ mutant. Removing a single point, or altering the value of a point within the range of its error bars, can be sufficient to substantially change the Hill coefficient calculated for fitting that data set. Therefore, the values we derive for  $k_{cat}$ ,  $K_{1/2}$ , and particularly  $n$  must be considered approximate. As a result, the categorization of various mutants as exhibiting cooperative or noncooperative kinetics is not made objectively based on the value of the apparent Hill coefficient but rather subjectively based on the shape of the best-fit curve.

## RESULTS

**Intragenic suppressor substitutions of *cheZ21IT* spanned the CheZ four-helix bundle.** To investigate the mechanism by which residues distant from the active site affect CheZ activity, intragenic suppressors of the *cheZ21IT* GOF phenotype were generated in a DNA repair-deficient strain. Potential mutants were screened phenotypically for the restoration of chemotaxis (Table 1), and plasmids were isolated from chemotactic mutants and sequenced. From the 18 chemotactic mutants isolated, 10 intragenic suppressor mutations were identified (*cheZ58VA*, *cheZ65AT*, *cheZ72SN*, *cheZ74EK*, *cheZ79HY*, *cheZ83MV*, *cheZ134EG*, *cheZ144LF*, *cheZ159IN*, and *cheZ163LS*). Four of the 10 mutations were isolated multiple times. All the suppressor mutations caused amino acid substitutions that were located along the CheZ four-helix bundle (Fig. 1). However, none were near the original GOF substitution site. The suppressor substitutions could be put into four groups based on their locations. The first group included substitutions 83MV and 79HY, which are located closest to the hairpin turn (or furthest from the original GOF substitution site) (Fig. 1). Although separated from each other by one alpha-helical turn, the side chains are long enough that Met83 points toward the interior of the four-helix bundle, whereas His79 points outward into solution. The next group contained substitutions 74EK, 72SN, and 134EG located in very close proximity to each other. These residues point in completely different directions: Glu74 points toward the nearby CheYp, Ser72 points inward into the four-helix bundle, and Glu134 points out into solution. A third group was close to the active

site and included substitutions 65AT, 58VA, and 144LF. Both Ala65 and Val58, which are separated from each other by two alpha-helical turns, point toward the center of the four-helix bundle. Leu144, which is one alpha-helical turn from the CheZ catalytic residue Gln147, points outward toward bound CheYp. Substitution 144LF is adjacent to a CheZ-CheYp stabilizing residue, Asp143, which interacts directly with CheYp (41). The final group, at the linker-proximal end of the four-helix bundle, included substitutions 159IN and 163LS, which are separated from each other by one alpha-helical turn. Both Ile159 and Leu163 point into the center of the four-helix bundle.

**Suppressor substitutions supported a range of chemotaxis phenotypes in the absence of CheZ21IT.** Following the phenotypic screening and identification of the suppressor substitutions (in the *cheZ21IT* background), suppressor mutations were generated in the wild-type *cheZ* background and assessed for their impact on chemotaxis. Mutants expressing the suppressor mutations alone demonstrated a wide range of swarm phenotypes, including wild type (Table 1). Substitutions 79HY, 83MV, 159IN, and 163LS, located furthest from the active site, were phenotypically silent and exhibited no significant swarming defects. Substitutions 72SN, 74EK, and 134EG, located proximal to each other and to sites of CheYp interaction, had strikingly different effects on swarm rates that ranged from 5 to 79% of wild-type rates. Suppressor substitutions 58VA, 65AT, and 144LF, near the catalytic residue Gln147, also supported swarm rates ranging from nonchemotactic to nearly wild type (8 to 75%). To determine if these swarm rates were due to altered intracellular CheZ concentrations, crude lysates of mutants chosen for further analysis (see below) were subjected to Western blot analysis to quantify the amount of CheZ present. CheZ expression by the five suppressor mutant strains assayed was similar to that of the *cheZ21IT* GOF strain (data not shown), suggesting that the swarm rate effects were due to changes in CheZ function rather than concentration.

**Suppressor substitutions were not allele specific.** Interestingly, 9 of the 10 suppressor substitutions also successfully suppressed the swarm phenotype of a different GOF mutation, *cheZ24LP* (26) (Table 1), based on nearly 100% wild-type

swarm rates for the double mutants. The remaining substitution, 72SN, significantly enhanced the swarm rate while not fully restoring chemotaxis. The lack of allele specificity demonstrated by the suppressor substitutions suggested that the mechanism of suppression did not involve a direct interaction between the original GOF and suppressor substitutions, which is consistent with the disparate locations of the substitutions along the four-helix bundle (Fig. 1). Furthermore, the ability of each suppressor to suppress two different GOF substitutions suggests that these GOF substitutions activate CheZ via a similar mechanism.

**Suppressor mutants exhibited various phosphatase activity profiles.** The direction of rotation of the *Escherichia coli* flagellar motor, and hence the swimming behavior of the cell, exhibits a cooperative dependence on CheYp concentration with a Hill coefficient of about 10 and therefore is exquisitely sensitive to changes in CheYp (8). Previous studies identified GOF and loss-of-function mutations in *cheZ* that increase or decrease phosphatase activity, respectively, either of which results in the loss of chemotaxis (4, 15, 25, 26, 35). In addition, a reduction in CheZ phosphatase activity at low CheYp levels appears to be required for successful chemotaxis (32). Thus, the increased phosphatase activity demonstrated by CheZ21IT at (physiologically) low CheYp concentrations (32) likely precludes chemotaxis. If the suppression of *cheZ21IT* was achieved by lowering the activity of CheZ21IT, especially at low concentrations of CheYp, then several different mechanisms of suppression (see Fig. 3A) are possible alone or in combination, including (i) the reduced binding of CheYp substrate, (ii) the reduced catalysis of the phosphatase reaction, and/or (iii) the restoration of the positive cooperativity of phosphatase activity exhibited by wild-type CheZ. To distinguish between these possibilities, five suppressor mutants that demonstrated a range of chemotaxis phenotypes (Table 1) and locations along the CheZ four-helix bundle (Fig. 1) were chosen for further analysis. Proteins containing the *cheZ21IT* suppressor substitution 72SN, 74EK, 134EG, 144LF, or 163LS expressed either alone in the wild-type *cheZ* background (single mutants) or in the *cheZ21IT* (double mutant) background were purified and assayed for phosphatase activity. The single-mutant data are described first.

The results produced by the  $P_i$  release assay are noisy, because the concentration of the substrate CheY113APp cannot be directly measured but instead is inferred, and multiple corrections and calculations are necessary to convert the experimental data into an interpretable form (see Materials and Methods). One indicator of this noise is the derivation of Hill coefficients that in some cases exceed the maximum value of 2 expected for a dimeric enzyme. Nevertheless, three distinct profiles of phosphatase activity could be distinguished among single suppressor mutants compared to wild-type CheZ. (i) Mutants CheZ74EK and CheZ144LF exhibited minimal (if any) phosphatase activity under the conditions tested (Fig. 2A) and did not support chemotaxis (Table 1). Because of very low activity, it was not possible to accurately determine kinetic values from the data available for these mutants. (ii) CheZ72SN and CheZ134EG exhibited apparent positive cooperativity (sigmoidal curves) as observed for wild-type CheZ (Fig. 2A), but their activities were shifted to higher concentrations of CheYp than that of wild-type CheZ, sug-

gesting a reduction in CheYp binding. The maximal reaction rates ( $V_{max}$ ), and thus  $k_{cat}$  for CheZ72SN and CheZ134EG, were nearly equivalent and reduced by about 2-fold compared to that of the wild-type CheZ (Table 2). (iii) Like CheZ21IT, CheZ163LS demonstrated apparently noncooperative phosphatase activity that was increased at low concentrations of CheYp compared to that of wild-type CheZ (Fig. 2A). Unlike CheZ21IT, however, CheZ163LS demonstrated wild-type swarming (Table 1), perhaps as a result of a 2-fold reduction in  $k_{cat}$  relative to that of CheZ21IT (Fig. 2A and Table 2). The phosphatase activities resulting from the suppressor substitutions correlated fairly well with the swarm rates of the single suppressor mutants: swarm rates increased as phosphatase activity increased (Fig. 2A and Table 1). This observation is consistent with successful chemotaxis requiring a finite but modest amount of phosphatase activity at low CheYp concentrations (32).

**Decreased catalysis, reduced substrate binding, and restoration of positive cooperativity can contribute to suppression of *cheZ21IT*.** All of the suppressor substitutions reduced CheZ21IT activity at low CheYp concentrations (0 to 0.2  $\mu$ M) to similar levels that were at or near that of wild-type CheZ (Fig. 2B, circled area). However, the phosphatase activities of double mutants bearing suppressor substitutions in the *cheZ21IT* background varied at higher CheYp concentrations (Fig. 2B), which suggested that suppression was accomplished via different mechanisms (Fig. 3A).

Because CheZ21IT has an alteration that results in an increased binding affinity for CheYp (32), mutants might achieve the suppression of CheZ21IT phosphatase activity by impeding binding to CheYp. Suppression by this mechanism should shift the phosphatase activity curve to higher CheYp concentrations (Fig. 3A, hypothesis i). *cheZ74EK* appeared to suppress *cheZ21IT* in just this manner and reduced phosphatase activity to nearly wild-type levels for a range of CheYp concentrations (Fig. 3B and Table 2), but this activity appeared to be noncooperative. Moreover, in the wild-type background, CheZ74EK demonstrated very low phosphatase activity, but its activity was rescued when expressed in the *cheZ21IT* background (Fig. 3B and Table 2). This further suggests that CheZ74EK has a substantial CheYp binding defect that is consistent with the location of the 74EK substitution as a surface residue in the central portion of the CheZ four-helix bundle (Fig. 1). No interaction between CheZ Glu74 and CheY was observed in the CheZ · CheY cocrystal structure; however, the electron density observed for much of CheY was poor (41).

The suppression of *cheZ21IT* also might occur by slowing the catalysis of the phosphatase reaction, which would lower the maximum rate of  $P_i$  release achieved (Fig. 3A, hypothesis ii) and would affect activity at low concentrations of CheYp. *cheZ144LF* and *cheZ163LS* suppressed CheZ21IT phosphatase activity to levels well below that of wild-type CheZ (Fig. 3C and Table 2) except at very low CheYp concentrations. Moreover, double-mutant combinations that include CheZ21IT provided only minimal enhancement of phosphatase activity compared to the CheZ144LF single mutant and substantially reduced phosphatase activity compared to the CheZ163LF single mutant (Fig. 3C). These results suggest that unlike CheZ74EK, the dominant defects of CheZ144LF and CheZ163LS were reduced catalysis of the phosphatase reac-

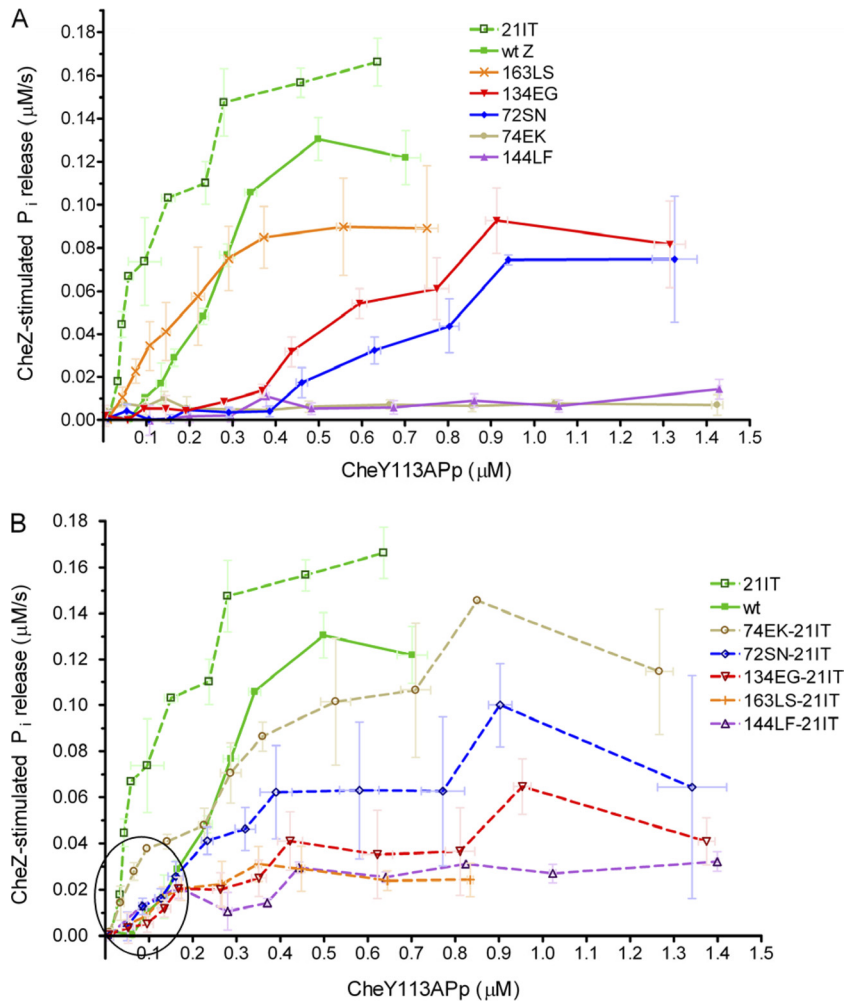


FIG. 2. Phosphatase activity measurements. CheZ proteins containing suppressor substitutions were purified and assessed for phosphatase activity. The calculated rate of  $P_i$  release ( $\pm$ SD) stimulated by CheZ is shown as a function of the calculated CheY113APp concentration ( $\pm$ SD) at steady state. (A) CheZ single mutants bearing suppressor substitutions alone. (B) CheZ double mutants bearing 21IT and suppressor substitutions. The circle in panel B highlights the decreased phosphatase activity exhibited by the double mutants at low substrate concentrations compared to the activity of CheZ21IT.

TABLE 2. Phosphatase activity kinetic constants for *cheZ* suppressors of 21IT as single mutants or as double mutants with 21IT

CheZ type	Kinetic constant <sup>a</sup>		<i>n</i> , apparent Hill coefficient
	$k_{\text{cat}}$ ( $\text{s}^{-1}$ )	$K_{1/2}$ ( $\mu\text{M}$ )	
Wild-type	$2.7 \pm 0.2$	$0.25 \pm 0.02$	3.5
21IT	$3.8 \pm 0.6$	$0.13 \pm 0.05$	1.2
74EK	ND <sup>b</sup>	ND	ND
74EK-21IT	$2.8 \pm 0.9$	$0.30 \pm 0.2$	1.2
144LF	ND	ND	ND
144LF-21IT	$1.0 \pm 1$	$0.71 \pm 3$	0.64
163LS	$1.9 \pm 0.5$	$0.17 \pm 0.07$	1.7
163LS-21IT	$0.5 \pm 0.1$	$0.11 \pm 0.03$	2.8
72SN	$1.6 \pm 0.4$	$0.72 \pm 0.2$	3.6
72SN-21IT	$1.5 \pm 0.4$	$0.21 \pm 0.1$	2.1
134EG	$1.7 \pm 0.2$	$0.53 \pm 0.07$	3.6
134EG-21IT	$0.9 \pm 0.3$	$0.25 \pm 0.2$	1.7

<sup>a</sup> The values listed are  $\pm$  standard deviations from a nonlinear regression fit of the data.

<sup>b</sup> ND indicates that values could not be accurately determined due to extremely low phosphatase activity under the experimental conditions employed.

tion, and impaired binding to CheYp did not make important contributions to the suppression of *cheZ21IT*. In the case of CheZ21IT163LS, reduced phosphatase activity at low CheYp concentrations also appears to be due to the restoration of cooperativity (hypothesis iii). CheZ163LS is the only one of the five suppressor substitution mutants measured for which the addition of the 21IT GOF substitution increased the estimated Hill coefficient (Table 2) and reduced rather than enhanced phosphatase activity at low CheYp concentrations.

The remaining suppressor substitutions did not fall clearly into a single category but instead affected both substrate binding (hypothesis i) and catalysis (hypothesis ii). CheZ72SN and CheZ134EG suppressed CheZ21IT phosphatase activity to levels below that of wild-type CheZ (Fig. 3D) and also reduced CheYp binding affinity to near the wild-type value (Table 2). Reductions in substrate binding and catalysis also were observed in the CheZ72SN and CheZ134EG single suppressor mutants. Interestingly, the mechanism of *cheZ21IT* suppression was not the restoration of cooperativity (hypothesis iii),

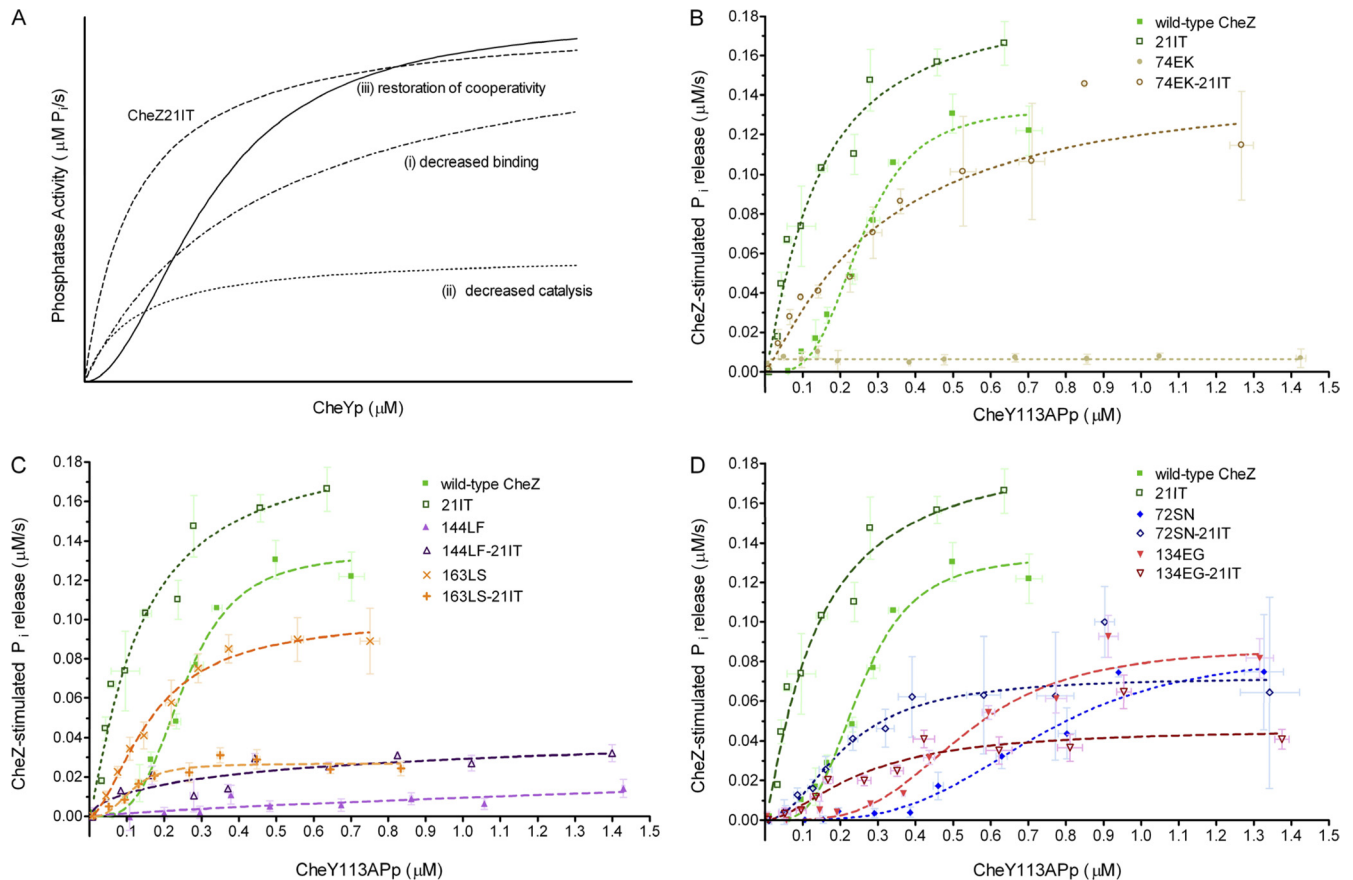


FIG. 3. Phosphatase activity comparisons. (A) Predicted phosphatase activity profiles for various mechanisms of *cheZ21IT* suppression. (B to D) Nonlinear regressions (shown as dashed lines) of the data shown in Fig. 2 calculated with Prism software using the Hill equation. Regressions for wild-type CheZ and CheZ21IT are compared to single and double CheZ mutants bearing the following suppressor substitutions alone or in combination with 21IT: 74EK (B), 144LF or 163LS (C), or 72SN or 134EG (D). As described in the legend to Fig. 2, the calculated rate of  $P_i$  release ( $\pm$ SD) stimulated by CheZ is shown as a function of calculated CheY113APp concentration ( $\pm$ SD) at steady state.

even though CheZ72SN and CheZ134EG were the only proteins among the five single suppressor mutants tested that retained cooperativity.

**Effects of suppressor and gain-of-function substitutions on CheZ activity are not due to altered dimerization.** One potential explanation for how amino acid substitutions far from the active site could affect CheZ activity is that CheZ monomers are inactive and the substitutions altered the CheZ monomer/dimer equilibrium. Such a hypothesis is consistent with the location of many substitutions at the dimer interface. However, the available data are inconsistent with the hypothesis that diminished CheZ activity is the result of a decrease in the fraction of dimers in the CheZ population. First, in preliminary experiments before choosing the assay conditions used in this study, the rate of  $P_i$  release from a saturating (6  $\mu$ M) concentration of CheY was measured as a function of CheZ concentration (50 to 760 nM) for wild-type CheZ, the gain-of-function mutants CheZ21IT and CheZ24LP, the suppressor mutants CheZ72SN, CheZ74EK, CheZ134EG, and CheZ144LF, and double mutants containing the 21IT substitution with each of the four listed suppressor mutants. In each case, the rate of  $P_i$  release per unit of concentration of CheZ (i.e., specific activity) was constant from 50 nM to at least 150 nM CheZ (and in

some cases much higher concentrations) (data not shown). In every case, the specific activity appears to decrease at high CheZ concentrations, as would be expected when CheY autophosphorylation becomes limiting, and the increase in specific activity at higher CheZ concentrations predicted by the monomer/dimer hypothesis was never observed. Second, the phosphatase activities of the various CheZ proteins (Table 2) correlated well with the chemotactic swarm rates of cells expressing the mutants (Table 1). The *in vitro* measurements were made at  $\sim$ 50 nM CheZ, whereas the *in vivo* concentration of CheZ depends on growth conditions but is  $\sim$ 1 to 30  $\mu$ M (16, 17, 19, 28). The consistent properties exhibited by CheZ at very different protein concentrations directly contradict the monomer/dimer hypothesis.

**DISCUSSION**

Bacterial chemotaxis depends on the appropriate modulation of CheYp concentration, which in turn depends on the stimulation of CheYp dephosphorylation by CheZ to an appropriate extent (not too much or too little). The *cheZ21IT* gain-of-function mutant lacks cooperativity, is hyperactive at low CheYp concentrations, and hence is nonchemotactic. Ten

suppressor substitutions that restore chemotaxis to *cheZ21IT* were located along the length of the CheZ four-helix bundle (Fig. 1). Nine of the substitutions also could suppress a different GOF mutation, *cheZ24LP* (Table 1). In the absence of a GOF substitution, the suppressor substitutions supported a range of chemotaxis phenotypes (Table 1). The suppressor substitutions altered CheZ phosphatase activity at low CheYp concentrations by reducing CheYp binding, reducing  $k_{cat}$ , and/or by increasing cooperativity (Table 2 and Fig. 2 and 3). To interpret the CheZ GOF suppressor mutant data reported here, it is useful to first provide the appropriate context by summarizing previously published data on the binding of CheYp to CheZ, cooperativity of CheZ activity, and CheZ GOF mutants.

**Cooperativity and binding of CheYp to CheZ.** One CheZ<sub>2</sub> dimer can bind and stimulate the dephosphorylation of two molecules of CheYp. The rate of release of phosphoryl groups from CheYp is a sigmoidal (cooperative) function of CheYp concentration when stimulated by wild-type CheZ but is a hyperbolic (noncooperative) function of CheYp concentration when stimulated by a CheZ GOF mutant (3, 32). A computational model makes an excellent fit to the experimental data by assuming (i) the association rate of the second CheYp to wild-type CheZ is about 40 times faster than the rate of the association of the first CheYp, and (ii) the rate of association for the second CheYp to wild-type CheZ and the rates of association for the first and second CheYp molecules to the CheZ21IT GOF mutant are all the same (32). Thus, the model suggests that the rate of the binding of the first CheYp to wild-type CheZ is somehow diminished, and this inhibition can be relieved either by binding CheYp or by GOF substitutions. In this view, the GOF substitutions actually result in the gain of CheZ function via the loss of the inhibition of CheYp binding.

Each of the two CheYp molecules binds directly to two distinct regions of CheZ, the C helix and the active-site region of the four-helix bundle (41). CheYp can bind to a peptide comprising the CheZ C helix alone with micromolar affinity (2, 20) but does not detectably associate with a truncated version of CheZ lacking the C helix (2, 41). The large difference in affinities of the two regions of CheZ for CheYp strongly suggests that CheYp binds first to the C helix of intact CheZ, and the increased local concentration of CheYp resulting from this tethering then facilitates the binding of CheYp to the CheZ active site. However, the data described do not reveal which interaction (with the C helix or the active site) is rate limiting for the association of CheYp with CheZ and hence is responsible for cooperativity.

**Cooperativity and CheZ gain-of-function mutants.** CheZ GOF mutants have been isolated using three different genetic screens: (i) the restoration of chemotaxis in bacteria bearing flagellar switches biased in the direction of rotation that is caused by high concentrations of CheYp identified CheZ GOF mutants with enhanced phosphatase activity (15, 35) and hence presumably reduced CheYp concentration; (ii) the restoration of chemotaxis in bacteria bearing a mutant CheY with reduced binding affinity for CheZ identified CheZ GOF mutants with enhanced binding to CheY (26); and (iii) additional CheZ GOF mutants were identified in bacteria that rotated their flagella in the direction caused by low CheYp concentrations (25). Altogether, 22 CheZ GOF substitutions were found in 18

different positions, and position 166 was hit in all three screens. Remarkably, only one GOF substitution (at the C terminus) could plausibly interact directly with CheYp. All of the other GOF substitutions are clustered together on the CheZ structure either in the N helix (at positions 17 to 29) or the nearby portions of the four-helix bundle (in positions 37 to 54 or 152 to 170). Although only two CheZ GOF mutants (CheZ21IT in the N helix and CheZ54RC in the four-helix bundle) have been shown to lack cooperativity, the observations that (i) all GOF mutants that have been tested lack cooperativity, (ii) GOF substitutions isolated in three different screens on the basis of enhanced phosphatase activity and/or enhanced CheY binding cluster in the same regions of the CheZ structure, and (iii) nine different substitutions that all suppress the nonchemotactic phenotype of one noncooperative GOF mutation also all restore chemotaxis to another GOF mutant (Table 1) are consistent with the simplifying assumption that all reported CheZ GOF substitutions (except 214FL at the C terminus) enhance CheZ activity by the same mechanism of relieving the inhibition of the binding of the first CheYp to CheZ<sub>2</sub> and eliminating cooperativity.

**Genetic and biophysical evidence suggests that cooperativity arises at the CheZ active site.** How then might GOF substitutions distant from the active site relieve the inhibition of binding of the first CheYp to CheZ<sub>2</sub>? Several hypotheses can be considered.

If the C helices or the adjacent linkers of CheZ interact with the N helix or nearby portions of the four-helix bundle, then the C helices might have diminished availability for CheYp binding. In this scenario, the GOF substitutions would release the C helices from such interactions. However, fluorescence anisotropy measurements indicate that the C helices of CheZ are fully mobile in the absence of CheYp (31), contrary to the predictions of this hypothesis. A related scheme that preserves the mobility of the CheZ C terminus would be if the two linkers or C helices within a CheZ dimer interacted with one another. The binding of CheYp to one C helix then would free the other C helix for enhanced binding to a second CheYp. However, this hypothesis predicts that GOF substitutions should occur in the C helix or linker, where they could directly disrupt the postulated self interaction, whereas almost all GOF substitutions actually are located in the N helix and nearby portions of the four-helix bundle. If the rate-limiting aspect of the first CheYp binding to CheZ (and hence the source of cooperativity) is association with the C helix, then it is difficult to envision how the known GOF substitutions could influence CheYp binding.

Another class of possibilities is that the rate-limiting step in the binding of CheYp to CheZ is association with the CheZ active site, even if CheYp first binds to the C helix of CheZ in a rapid equilibrium. It has been suggested that in the absence of CheYp, the N helices of CheZ fold along the four-helix bundle and occlude the active site (41). In this circumstance, the GOF substitutions would disrupt interactions between the N helices and the four-helix bundle, thus permitting access to the active site. Similarly, in such a model CheYp binding to the CheZ active site would displace both N helices. However, fluorescence anisotropy measurements indicate that the mobility of the N helices is not substantially different in the pres-



ence or absence of CheYp (31), contrary to the predictions of this hypothesis.

The hypothesis most consistent with available evidence is that the binding of CheYp to the CheZ active site is indeed the rate-limiting step for association, and that cooperativity results because the binding of the first CheYp changes the conformation of the other CheZ active site on the opposite side of the four-helix bundle. Consistent with this model, a kink in the CheZ four-helix bundle in the vicinity of the bound CheY · BeF<sub>3</sub><sup>-</sup> (41) may be a consequence of CheYp binding. In this model for positive cooperativity, the CheZ GOF substitutions such as 21IT would be predicted to result in structural or dynamic effects that propagate along the four-helix bundle and change the features of the active sites that slow down the binding of the first CheYp to wild-type CheZ. The CheZ21IT suppressor substitutions dampen this enhanced activity, either by directly or indirectly reducing CheYp binding and/or catalysis. Indirect effects of suppressors located far from the active site could occur via a similar mechanism of transmission through the four-helix bundle. Several observations support this proposed mechanism for the GOF mutants and their suppressors. First, there is direct nuclear magnetic resonance evidence for the propagation of structural changes along the CheZ four-helix bundle upon the binding of the CheA<sub>S</sub> protein to the hairpin end (7, 13). Furthermore, CheA<sub>S</sub> has been reported to enhance CheZ activity about 2-fold (21, 40), an enhancement similar in magnitude to that exhibited by GOF mutants, thus raising the possibility that structural changes in the bundle affect CheZ activity. However, it is not known whether CheA<sub>S</sub> binding relieves CheZ cooperativity. The effect of CheA<sub>S</sub> was observed using assay conditions (4°C, 0.1 mM Mg<sup>2+</sup>, 4 nM CheZ, and 1 nM CheA<sub>S</sub>) under which CheZ stimulated the rate of CheYp dephosphorylation by 40% (21, 40). Under the assay conditions used in this work (room temperature, 10 mM Mg<sup>2+</sup>, and 50 nM CheZ), CheZ stimulates CheYp dephosphorylation 100-fold (32). Under very similar conditions (100 instead of 50 nM CheZ), the addition of CheA<sub>S</sub> equimolar to CheZ had no further effect (E. Schilling and R. E. Silversmith, unpublished results). Second, all 10 of the suppressor substitutions reported in this study are found on the CheZ four-helix bundle on either side of the active site, and most have side chains that insert into the interior of the four-helix bundle. The suppressors thus are positioned either within the active site or at positions that could cause perturbations to propagate from their location to the active site. The complete absence of suppressor substitutions in the C helix or adjacent linker further suggests that the impact of the original GOF substitution is not on the C helix, and therefore that the key step for cooperativity is binding to the active site. Finally, before the present study, some GOF substitutions were known to affect CheYp binding at a distance (26). However, the alteration of CheYp binding cannot be unambiguously interpreted, because two different regions of CheZ interact with CheYp. Those GOF mutants known to increase CheZ phosphatase activity were not characterized in sufficient detail to distinguish whether CheYp binding or the catalysis of the dephosphorylation reaction was affected. However, the present work shows that several suppressor substitutions affect the catalysis of dephosphorylation (Table 2) and therefore almost certainly affect the active site from a distance.

In summary, the preponderance of available evidence suggests that CheYp first binds to the C helix of CheZ, the second step of CheYp binding (to the CheZ active site) is rate limiting, and the cooperativity of CheZ phosphatase activity arises from properties of the CheZ active site. Furthermore, CheZ GOF and suppressor substitution mutants can influence active-site properties (CheYp binding and the catalysis of dephosphorylation) from a distance, possibly via structural or dynamic changes that propagate through the CheZ structure from the site of substitution to the active site.

#### ACKNOWLEDGMENTS

We thank Doug Whitfield for constructing plasmids encoding seven *cheZ24LP* suppressor double mutations and assaying the chemotaxis of the resulting mutants, Yael Pazy and Stephanie Thomas for helpful discussions, and Bob Immormino for the thoughtful review of the manuscript. Insightful suggestions by the anonymous peer reviewers concerning dimerization, Hill coefficients, and CheA<sub>S</sub> led to improvements in the manuscript.

Although the project described herein was supported by grants GM050860 (to R.B.B.) and 5K12GM000678 (to SPIRE) from the National Institute of General Medical Sciences, its contents are solely the responsibility of the authors and do not necessarily represent the official views of the National Institute of General Medical Sciences or the National Institutes of Health.

#### REFERENCES

- Appleby, J. L., and R. B. Bourret. 1998. Proposed signal transduction role for conserved CheY residue Thr87, a member of the response regulator active-site quintet. *J. Bacteriol.* **180**:3563–3569.
- Blat, Y., and M. Eisenbach. 1996. Conserved C-terminus of the phosphatase CheZ is a binding domain for the chemotactic response regulator CheY. *Biochemistry* **35**:5679–5683.
- Blat, Y., B. Gillespie, A. Bren, F. W. Dahlquist, and M. Eisenbach. 1998. Regulation of phosphatase activity in bacterial chemotaxis. *J. Mol. Biol.* **284**:1191–1199.
- Boesch, K. C., R. E. Silversmith, and R. B. Bourret. 2000. Isolation and characterization of nonchemotactic CheZ mutants of *Escherichia coli*. *J. Bacteriol.* **182**:3544–3552.
- Bourret, R. B., J. F. Hess, and M. I. Simon. 1990. Conserved aspartate residues and phosphorylation in signal transduction by the chemotaxis protein CheY. *Proc. Natl. Acad. Sci. U. S. A.* **87**:41–45.
- Bray, D., R. B. Bourret, and M. I. Simon. 1993. Computer simulation of the phosphorylation cascade controlling bacterial chemotaxis. *Mol. Biol. Cell* **4**:469–482.
- Cantwell, B. J., et al. 2003. CheZ phosphatase localizes to chemoreceptor patches via CheA-short. *J. Bacteriol.* **185**:2354–2361.
- Cluzel, P., M. Surette, and S. Leibler. 2000. An ultrasensitive bacterial motor revealed by monitoring signaling proteins in single cells. *Science* **287**:1652–1655.
- Degnen, G. E., and E. C. Cox. 1974. Conditional mutator gene in *Escherichia coli*: isolation, mapping, and effector studies. *J. Bacteriol.* **117**:477–487.
- Goldbeter, A., and D. E. Koshland, Jr. 1981. An amplified sensitivity arising from covalent modification in biological systems. *Proc. Natl. Acad. Sci. U. S. A.* **78**:6840–6844.
- Guhaniyogi, J., V. L. Robinson, and A. M. Stock. 2006. Crystal structures of beryllium fluoride-free and beryllium fluoride-bound CheY in complex with the conserved C-terminal peptide of CheZ reveal dual binding modes specific to CheY conformation. *J. Mol. Biol.* **359**:624–645.
- Guhaniyogi, J., T. Wu, S. S. Patel, and A. M. Stock. 2008. Interaction of CheY with the C-terminal peptide of CheZ. *J. Bacteriol.* **190**:1419–1428.
- Hao, S., D. Hamel, H. Zhou, and F. W. Dahlquist. 2009. Structural basis for the localization of the chemotaxis phosphatase CheZ by CheA<sub>S</sub>. *J. Bacteriol.* **191**:5842–5844.
- Hess, J. F., R. B. Bourret, and M. I. Simon. 1991. Phosphorylation assays for proteins of the two-component regulatory system controlling chemotaxis in *Escherichia coli*. *Methods Enzymol.* **200**:188–204.
- Huang, C., and R. C. Stewart. 1993. CheZ mutants with enhanced ability to dephosphorylate CheY, the response regulator in bacterial chemotaxis. *Biochim. Biophys. Acta* **1202**:297–304.
- Kuo, S. C., and D. E. Koshland, Jr. 1987. Roles of *cheY* and *cheZ* gene products in controlling flagellar rotation in bacterial chemotaxis of *Escherichia coli*. *J. Bacteriol.* **169**:1307–1314.
- Li, M., and G. L. Hazelbauer. 2004. Cellular stoichiometry of the components of the chemotaxis signaling complex. *J. Bacteriol.* **186**:3687–3694.

18. Liu, J. D., and J. S. Parkinson. 1989. Role of CheW protein in coupling membrane receptors to the intracellular signaling system of bacterial chemotaxis. *Proc. Natl. Acad. Sci. U. S. A.* **86**:8703–8707.
19. Matsumura, P., S. Roman, K. Volz, and D. McNally. 1990. Signalling complexes in bacterial chemotaxis. *Symp. Soc. Gen. Microbiol.* **46**:135–154.
20. McEvoy, M. M., A. Bren, M. Eisenbach, and F. W. Dahlquist. 1999. Identification of the binding interfaces on CheY for two of its targets, the phosphatase CheZ and the flagellar switch protein FliM. *J. Mol. Biol.* **289**:1423–1433.
21. O'Connor, C., and P. Matsumura. 2004. The accessibility of Cys-120 in CheA(S) is important for the binding of CheZ and enhancement of CheZ phosphatase activity. *Biochemistry* **43**:6909–6916.
22. Park, S. Y., et al. 2004. Structure and function of an unusual family of protein phosphatases: the bacterial chemotaxis proteins CheC and CheX. *Mol. Cell* **16**:563–574.
23. Parkinson, J. S. 1978. Complementation analysis and deletion mapping of *Escherichia coli* mutants defective in chemotaxis. *J. Bacteriol.* **135**:45–53.
24. Pazy, Y., et al. 2010. Identical phosphatase mechanisms achieved through distinct modes of binding phosphoprotein substrate. *Proc. Natl. Acad. Sci. U. S. A.* **107**:1924–1929.
25. Sanna, M. G., and M. I. Simon. 1996. *In vivo* and *in vitro* characterization of *Escherichia coli* protein CheZ gain- and loss-of-function mutants. *J. Bacteriol.* **178**:6275–6280.
26. Sanna, M. G., and M. I. Simon. 1996. Isolation and *in vitro* characterization of CheZ suppressors for the *Escherichia coli* chemotactic response regulator mutant CheYN23D. *J. Biol. Chem.* **271**:7357–7361.
27. Schaaper, R. M., and R. Cornacchio. 1992. An *Escherichia coli dnaE* mutation with suppressor activity toward mutator *mutD5*. *J. Bacteriol.* **174**:1974–1982.
28. Scharf, B. E., K. A. Fahrner, and H. C. Berg. 1998. CheZ has no effect on flagellar motors activated by CheY13DK106YW. *J. Bacteriol.* **180**:5123–5128.
29. Segall, J. E., M. D. Manson, and H. C. Berg. 1982. Signal processing times in bacterial chemotaxis. *Nature* **296**:855–857.
30. Silversmith, R. E. 2010. Auxiliary phosphatases in two-component signal transduction. *Curr. Opin. Microbiol.* **13**:177–183.
31. Silversmith, R. E. 2005. High mobility of carboxyl-terminal region of bacterial chemotaxis phosphatase CheZ is diminished upon binding divalent cation or CheY-P substrate. *Biochemistry* **44**:7768–7776.
32. Silversmith, R. E., M. D. Levin, E. Schilling, and R. B. Bourret. 2008. Kinetic characterization of catalysis by the chemotaxis phosphatase CheZ. Modulation of activity by the phosphorylated CheY substrate. *J. Biol. Chem.* **283**:756–765.
33. Silversmith, R. E., J. G. Smith, G. P. Guanga, J. T. Les, and R. B. Bourret. 2001. Alteration of a nonconserved active site residue in the chemotaxis response regulator CheY affects phosphorylation and interaction with CheZ. *J. Biol. Chem.* **276**:18478–18484.
34. Smith, J. G., et al. 2004. A search for amino acid substitutions that universally activate response regulators. *Mol. Microbiol.* **51**:887–901.
35. Sockett, H., S. Yamaguchi, M. Kihara, V. M. Irikura, and R. M. Macnab. 1992. Molecular analysis of the flagellar switch protein FliM of *Salmonella typhimurium*. *J. Bacteriol.* **174**:793–806.
36. Sourjik, V., and J. P. Armitage. 2010. Spatial organization in bacterial chemotaxis. *EMBO J.* **29**:2724–2733.
37. Szurmant, H., and G. W. Ordal. 2004. Diversity in chemotaxis mechanisms among the bacteria and archaea. *Microbiol. Mol. Biol. Rev.* **68**:301–319.
38. ThermoScientific. 2007. Western blotting handbook and troubleshooting guide. Thermo Fisher Scientific, Waltham, MA.
39. Thomas, S. A., J. A. Brewster, and R. B. Bourret. 2008. Two variable active site residues modulate response regulator phosphoryl group stability. *Mol. Microbiol.* **69**:453–465.
40. Wang, H., and P. Matsumura. 1996. Characterization of the CheA<sub>9</sub>/CheZ complex: a specific interaction resulting in enhanced dephosphorylating activity on CheY-phosphate. *Mol. Microbiol.* **19**:695–703.
41. Zhao, R., E. J. Collins, R. B. Bourret, and R. E. Silversmith. 2002. Structure and catalytic mechanism of the *E. coli* chemotaxis phosphatase CheZ. *Nat. Struct. Biol.* **9**:570–575.